

Supplementary Materials

In situ transformation of ZIF-67 into hollow $\text{Co}_2\text{V}_2\text{O}_7$ nanocages on graphene as high-performance cathode for aqueous asymmetric supercapacitors

Kai Le^a, Mengjiao Gao^b, Dongmei Xu^a, Zhou Wang^b, Guanwen Wang^b, Guixia Lu^c,

Wei Liu^{a, *}, Fenglong Wang^{b, *}, Jiurong Liu^{b, *}

^a State Key Laboratory of Crystal Materials, Institute of Crystal Materials, Shandong University, Shandong 250100, China

^b School of Materials Science and Engineering, Shandong University, Jinan, Shandong 250061, China

^c School of Civil Engineering, Qingdao University of Technology, Qingdao, Shandong 266033, China

*Corresponding author.

E-mail: weiliu@sdu.edu.cn (W. L.), fenglong.wang@sdu.edu.cn (F. W.), and jrliu@sdu.edu.cn (J. L.)

Calculation

The specific capacity (Q) of single electrode can be determined from GCD curves through formula:¹

$$Q = \frac{I \times \Delta t}{m} \quad (\text{S1})$$

where Δt , and I are the discharge time, the charge-discharge current, and the potential range excluding IR drop in charge-discharge curves, and m represents the mass loading of the working electrode.

For the ASC device, the mass ration of cathode and anode was determined by equation:²

$$\frac{m_+}{m_-} = \frac{Q_-}{Q_+} \quad (\text{S2})$$

where m and Q represents the mass loading and capacity of cathode (+) and anode (-), respectively. The specific capacitance, energy density, and power density of ASC device were calculated by formulas:³

$$C_{cell} = \frac{I \times \Delta t}{m \times \Delta V} \quad (\text{S3})$$

$$E = \frac{1}{2} C_{cell} \Delta V^2 \quad (\text{S4})$$

$$P = \frac{E}{\Delta t} \quad (\text{S5})$$

where C_{cell} , ΔV , and Δt are the corresponding parameters in discharge curves, and m represents the total mass loading of two electrodes in ASC device.

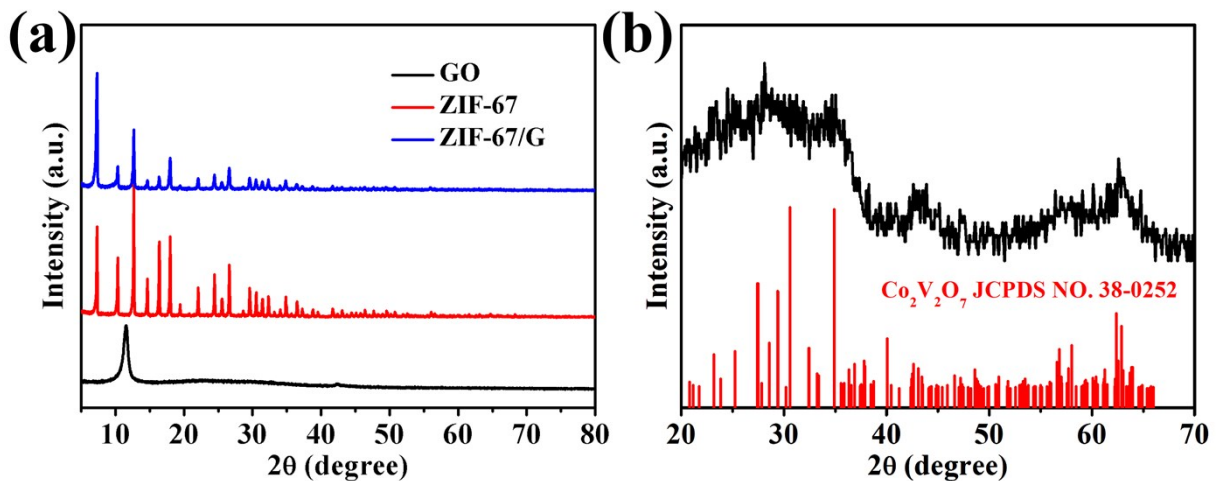


Fig. S1 (a) XRD patterns of GO, ZIF-67, and ZIF-67/G; (b) XRD patterns of Co₂V₂O₇/G.

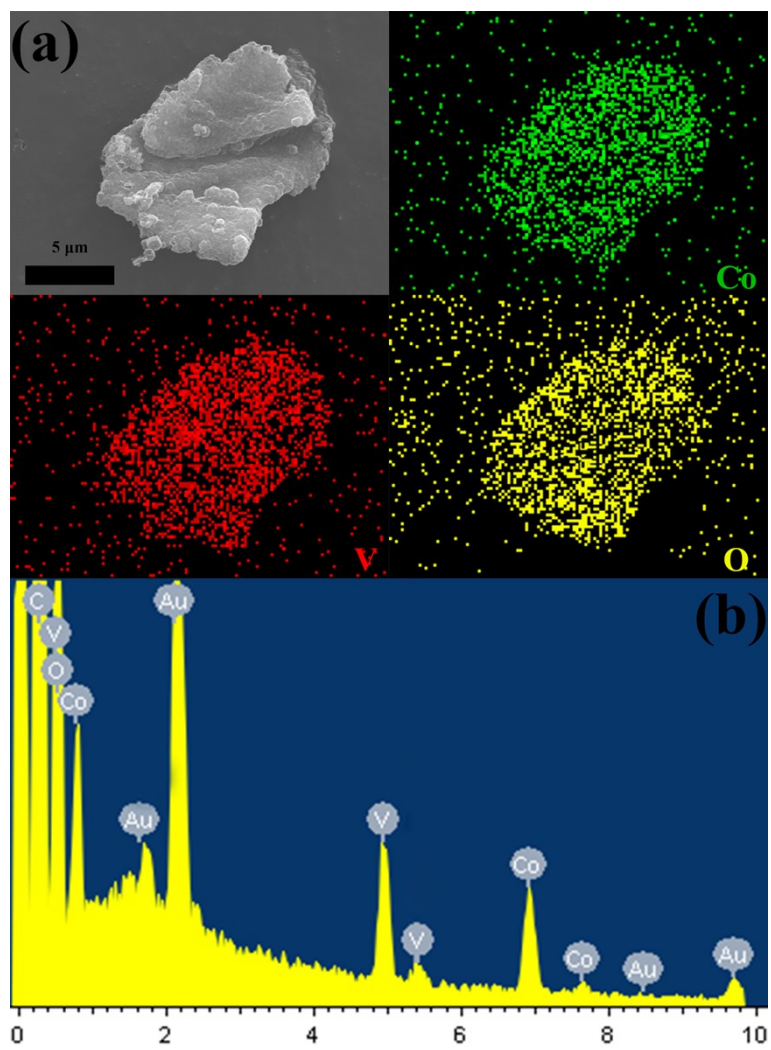


Fig. S2 (a) elemental mapping image and (b) EDX spectrum $\text{Co}_2\text{V}_2\text{O}_7/\text{G}$.

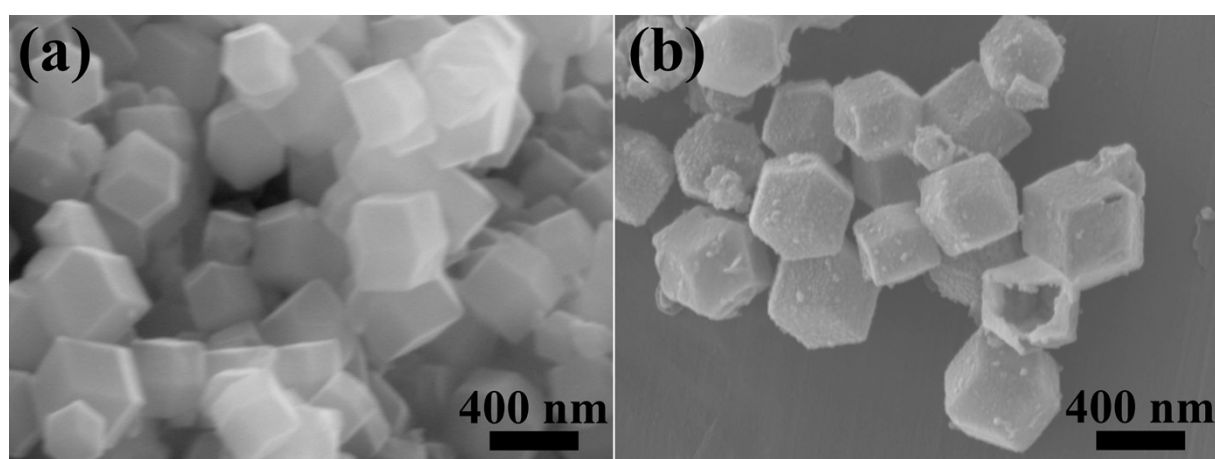


Fig. S3 SEM of (a) ZIF-67 and (b) $\text{Co}_2\text{V}_2\text{O}_7$.

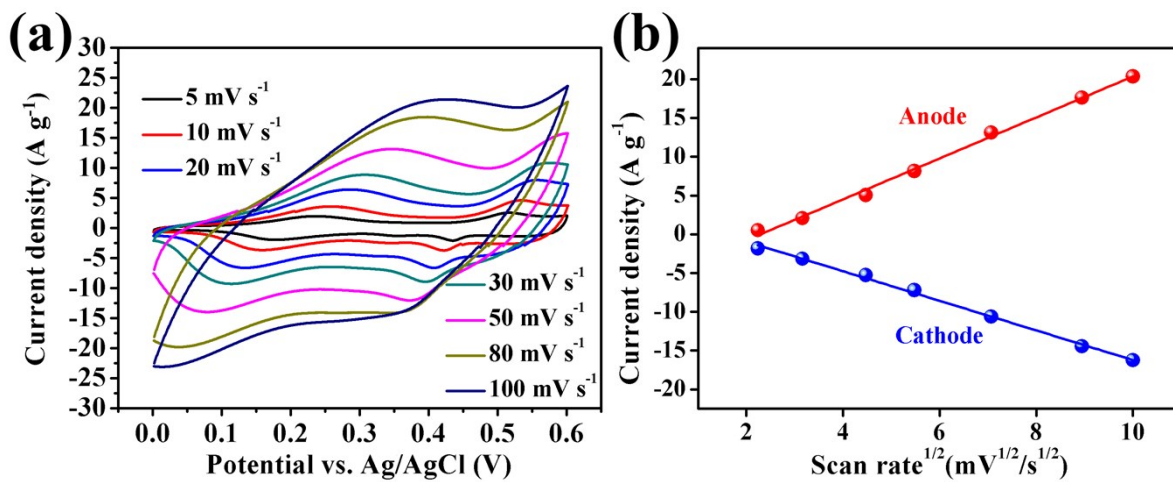


Fig. S4 (a) CV curves of the $\text{Co}_2\text{V}_2\text{O}_7$ electrode at different scan rates; (b) linear relationship between the anodic/cathodic peak currents at the square root of the scan rates.

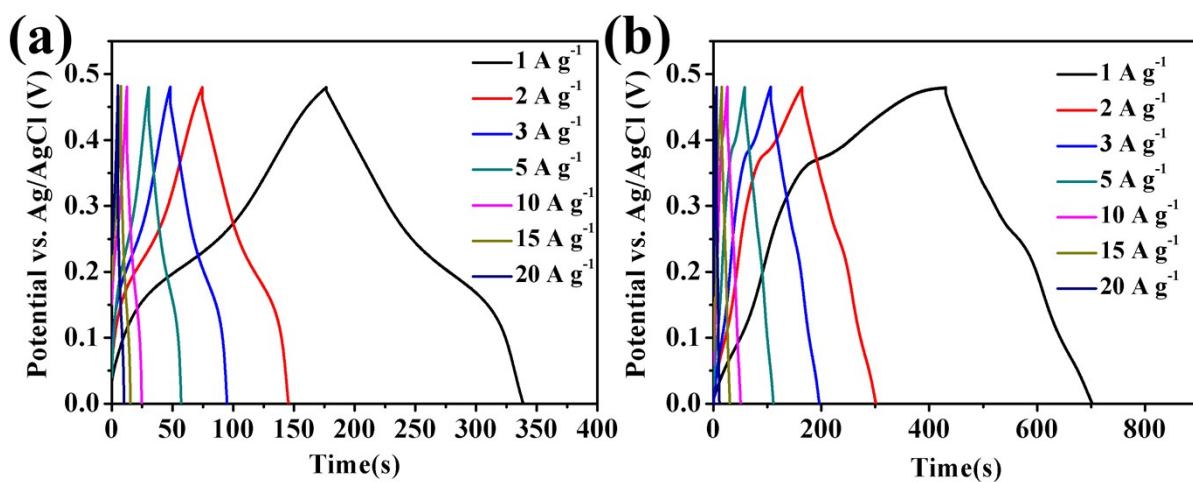


Fig. S5 GCD curves of (a) $\text{Co}_2\text{V}_2\text{O}_7$ and (b) $\text{Co}_2\text{V}_2\text{O}_7/\text{G}$ electrodes at different current densities.

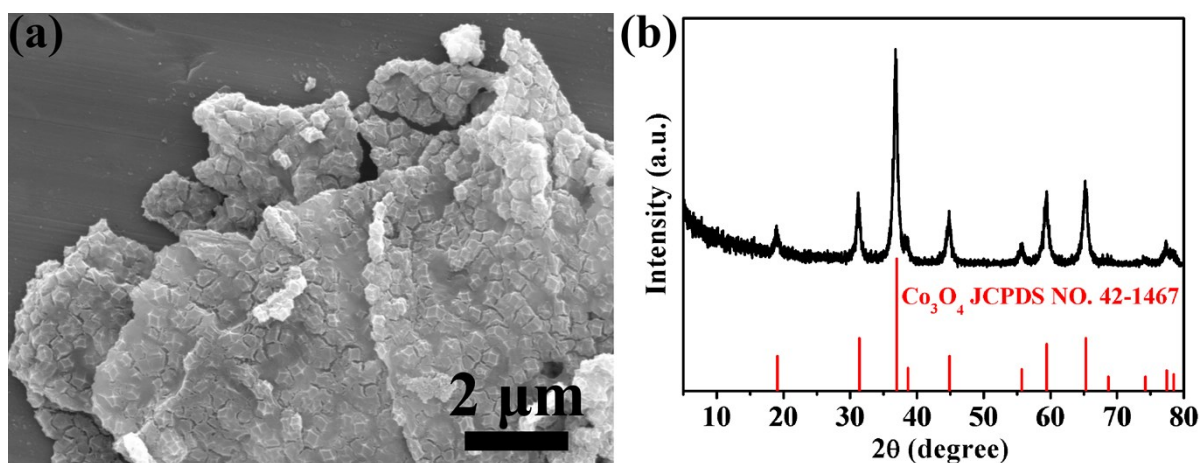


Fig.S6 (a) SEM and (b) XRD pattern of $\text{Co}_3\text{O}_4/\text{G}$ composites.

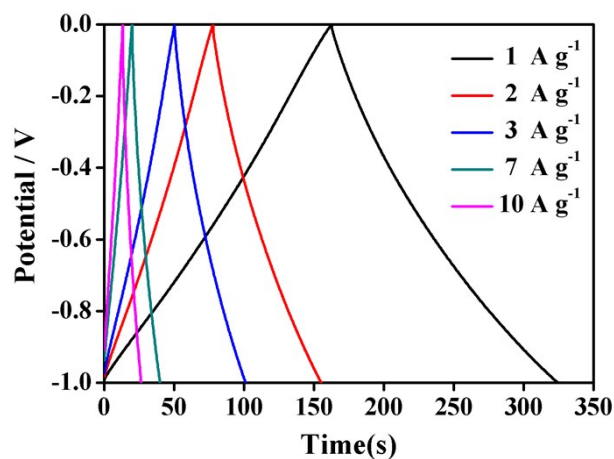


Fig. S7 GCD curves of rGO electrode at different current densities.

Reference

1. C. Qu, L. Zhang, W. Meng, Z. Liang, B. Zhu, D. Dang, S. Dai, B. Zhao, H. Tabassum, S. Gao, H. Zhang, W. Guo, R. Zhao, X. Huang, M. Liu and R. Zou, MOF-derived α -NiS nanorods on graphene as an electrode for high-energy-density supercapacitors, *J. Mater. Chem. A*, 2018, **6**, 4003-4012.
2. Y. Wen, S. Peng, Z. Wang, J. Hao, T. Qin, S. Lu, J. Zhang, D. He, X. Fan, G. Cao, Facile synthesis of ultrathin NiCo₂S₄ nano-petals inspired by blooming buds for high-performance supercapacitors, *J. Mater. Chem. A*, 2017, **5**, 7144-7152.
3. N. Liu, Y. Su, Z. Wang, Z. Wang, J. Xia, Y. Chen, Z. Zhao, Q. Li, F. Geng, Electrostatic-Interaction-Assisted Construction of 3D Networks of Manganese Dioxide Nanosheets for Flexible High-Performance Solid-State Asymmetric Supercapacitors, *ACS Nano*, 2017, **11**, 7879-7888.